PCCP

Accepted Manuscript

ROYAL SOCIETY OF CHEMISTRY

www.rsc.org/pccp

Cite this: DOI: 10.1039/c0xx00000x

www.rsc.org/xxxxxx

Communication

Temperature-induced Structural and Chemical Changes of Ultrathin Ethylene Carbonate Films on Cu(111)

Florian Buchner, [‡,a,b] Hanieh Farkhondeh, [‡,§,a,b] Maral Bozorgchenani, [‡,a,b] Benedikt Uhl,[a,b] and R. Jürgen Behm* [a,b]

Received (in XXX, XXX) Xth XXXXXXXXX 20XX, Accepted Xth XXXXXXXXX 20XX
DOI: 10.1039/b000000x

The interaction of the Li-ion battery solvent ethylene carbonate (EC) with Cu(111) was investigated by scanning tunnelling microscopy (STM) and variable temperature X-ray photoelectron spectroscopy (XPS) under ultrahigh vacuum (UHV) conditions. Between 80 K and 420 K, the decomposition of EC goes along with distinct structural and chemical changes in the adlayer.

The technological change from carbon based fossil energy fuels to renewable energy sources is the key for a sustainable energy system in the future. Sources like wind or solar energy are promising, but the energy generation is volatile and will result in temporal discrepancies between availability and demand. Consequently, highly efficient energy storage systems are urgently needed.[1] Meanwhile, the electrochemical energy storage in Lithium ion (Li-ion) batteries is indispensable for electronic devices, and due to their high energy density and long cycle life they are also promising candidates as power source for vehicles.[2,3] To improve the performance of Lithium ion batteries, much effort has been invested into the development of new electrode materials to improve energy density, charge/discharge rates, and lifetime.[4] In particular, studies have focussed on the solid–electrolyte interphase (SEI), which is formed on the surface of the electrode during the first operating cycle and mainly determines the batteries´ properties. It develops during the electrochemical reduction and subsequent decomposition of the organic solvent based electrolyte. Carbonates are the most frequently used solvents in commercial Li-ion batteries, with the electrolyte often being a mixture of ethylene carbonate (EC), propylene carbonate (PC), and linear carbonates, such as diethyl carbonate (DEC) or dimethylcarbonate (DMC), lithium salts, and other additives.[5]

Generally, it is challenging to derive a detailed understanding of the interactions and of the underlying mechanisms in multicomponent systems such as Li-ion batteries. Though numerous studies have been conducted *in situ*, in an electrochemical environment, details of the interaction of each component with the electrode, at the electrode|electrolyte interface, at a molecular level, are essentially unresolved.[6,7] Some insight was derived from spectroscopic studies. For example, Fourier transform infrared reflectance spectroscopy (FTIRS)[8] and Raman spectroscopy[9] were employed to probe the stability of carbonate solutions at different potentials. Very recently, Yu *et al.*[10] observed an enrichment of EC on the surface of a $LiCo_2O$ electrode out of a mixture of carbonates in a solution using SFG. These authors were also able to draw conclusions on the adsorption geometry of the solvent, in the absence of an applied potential difference. Under these conditions, the majority of EC molecules, about 60%, points with the carbonyl group toward the surface, with the carbonyl group being slightly tilted, while the minority fraction points toward the opposite direction. Besides these *in-situ* investigations in solution, also *ex-situ* measurements have been performed. The elemental composition of the electrode surface after cycling was characterized by X-ray photoelectron spectroscopy (XPS) and nuclear magnetic resonance (NMR).[11] Wang *et al.*[12] studied the temperature dependent behaviour of condensed layers of tetrahydrofuran and PC with thicknesses of more than 100 Å on Al(111) by XPS, showing that, *e.g.*, a fraction of the PC decomposes under loss of the carboxyl oxygen close to its melting point, followed by removal while upon increasing the temperature of the carbonyl oxygen at higher temperature, is removed until at room temperature no intact PC can be found.

In contrast to these experiments, which essentially probe the bulk behaviour of the electrolyte, only few experiments have been reported which focussed on the interaction of the electrolyte / solvent with the electrode, using very thin layers. Very recently, Becker *et al*. studied the reaction of DEC with $LiCoO_2$ electrodes by synchrotron radiation based XPS; they found a chemical adsorption of the monolayer on the electrode, followed by van der Waals type interactions in the multilayer regime.[13]

There is little information, however, on the structure and structure formation of these organic solvent molecules on the electrode surface, in the monolayer regime, and the same is true for details of the reactive interaction of the solvent molecules with the electrode, albeit the particular importance of molecular arrangements on smooth surfaces as explicitly discussed in literature. [14-18] This is topic of the present work, where we investigated the interaction of ethylene carbonate with Cu(111) under ultrahigh vacuum (UHV) conditions in the sub-monolayer to monolayer regime, in the range between 80 K and 420 K, focussing on the structure and structure formation and on reactive decomposition processes. The combination of STM imaging and XPS measurements allows to unambiguously

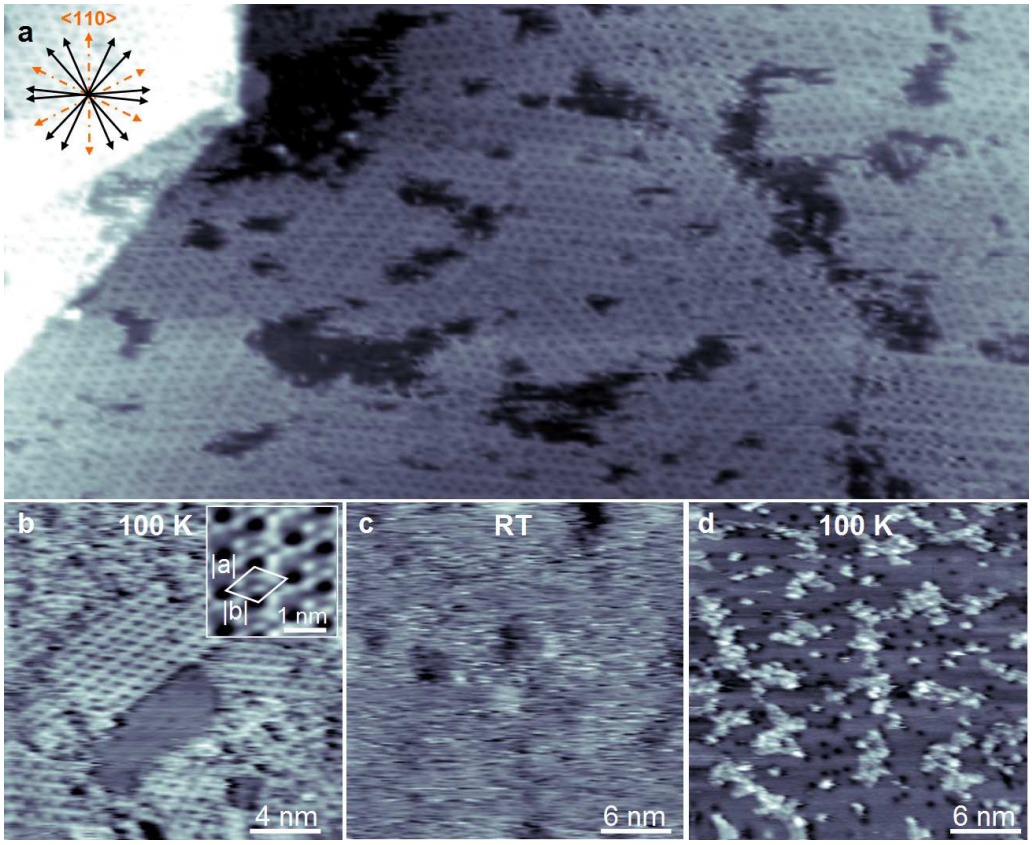

Figure 1. STM images of a Cu(111) surface covered by a submonolayer of EC, after deposition on the sample held at 80K. (a, b) STM images acquired at 112 K and 126 K, respectively, (c) STM image recorded upon heating to room temperature, and (d) STM image after subsequent cool down to 114 K, resolving stable islands coexistent with depressions associated with adsorbed oxygen (see text).

identify intact EC molecules on Cu(111) and resolve distinct chemical and structural changes of the adlayer at different temperatures. To the best of our knowledge, this is the first time that the interaction of EC molecules with model electrode surfaces has been studied in ultrathin films with techniques that are sensitive to changes in both structural and chemical surface properties at variable temperatures. We believe that such kind of model studies, characterizing the interaction of key components of electrolyte with model electrode surfaces, first individually and later in increasingly complex systems and under increasingly more realistic conditions, are essential for a fundamental understanding of the processes at the electrode|electrolyte interface and subsequently for the improvement of real battery applications.

STM measurements of submonolayer EC films on Cu(111) which were prepared by vapour deposition on the sample held at 80 K (Figure 1a and b), reveal that the molecules self-assemble into a well-ordered quasi-hexagonal (2D) EC network. (2D) EC islands exhibit six distinct azimuthal orientations (indicated by arrows in Figure 1a), *i.e.*, they are symmetrically aligned to each of the main directions of the underlying copper atomic lattice. In that medium resolution STM images no individual EC molecules are resolved. In the molecularly resolved STM image (see inset at a magnified scale in Figure 1b) the unit cell is drawn (length of the lattice vectors: 0.9 ± 0.1 nm). The protrusions are associated with individual EC molecules. Details on the arrangement will be discussed in a forthcoming publication. The areas around these (2D) EC islands appear either with lower height, due to the absence of EC admolecules, or noisy, which is indicative for mobile molecular adspecies diffusing too fast below the STM tip to be resolved.[19,20,21] In addition, we find massive changes at the boundary of the (2D) EC islands in consecutive STM images, *i.e.*, the island shape strongly changes with time, which can result from either attachment and/or detachment of molecules at the island perimeter or motion of adsorbed EC molecules along the island perimeter. Although high tunnelling resistances of ~ 10 – 70 GΩ were applied, tip effects can not be excluded. We assume that two-dimensional (2D) EC islands are in equilibrium with a (2D) gas/liquid phase, as observed similarly for other molecular species on smooth metal surfaces. The sizeable rate for admolecule detachment already at ~100 K indicates that the intermolecular interactions are relatively weak; in addition also the barrier for admolecule surface diffusion must be low. Assuming a flat lying configuration of EC the (2D) EC network is most likely stabilized by intermolecular hydrogen bonds.

Upon annealing to room temperature, the STM images show noisy features (Figure 1c), which is attributed to a molecular adspecies with a high mobility in the adlayer, which is too high on the time scale of the STM experiment. Annealing to room temperature and subsequent cool down to ~100 K (Figure 1d)

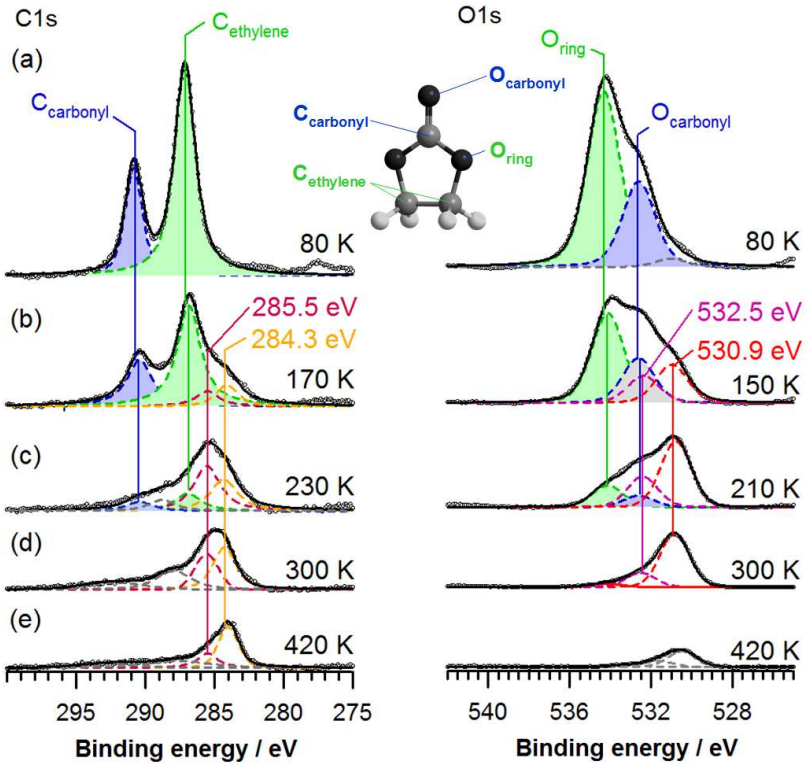

Figure 2. XP core level spectra in the C1s (a) and the O1s region (b), recorded of an EC covered Cu(111) surface during slow annealing at the temperatures indicated in the figure (T_{depos} = 80 K, initial EC coverage ca. 1.5 ML), which illustrate the thermally induced desorption and decomposition of the adsorbed EC species. In addition to the measured spectra, peaks related to different decomposition products are indicated (peak fitting procedure and interpretation see text).

leads to an irreversible transformation of the (2D) EC islands into islands with arbitrary shapes. These islands coexist with depressions in the areas in between. The depressions closely resemble those observed by Yang *et al*. and Wiame *et al*.[22,23] in the initial stages of copper oxidation. These authors interpreted bright rings with a central depression, randomly distributed over the Cu(111) surface as oxygen adatoms, which is typical for atomic oxygen on metal surfaces. This apparent lower height at these locations is due to an electronic effect, where charge transfer to the adatom depletes the local density of states at the adsorption site.[24] Thus we assume that the surface cavities shown in Figure 1c stem from adsorbed oxygen (O_{ad}), produced upon decomposition of EC. The areas in between these agglomerates appear less noisy than in Figure 1a and the branched island are much more stable, indicating that they also consist of molecular fragments of the decomposition process rather than of intact adsorbed EC molecules. Additional STM measurements after evaporation deposition of EC on the sample at 80 K, moderate heating to 180, 190 and around 200 K, respectively and subsequent cool down to ~100 K confirmed the resulting fragments, in particular O_{ad}. The presence of these immobile species is clearly resolved after the annealing step.

To support the structural information gained by STM, the chemical composition of the adlayer and changes therein were characterized by variable temperature XPS in the range between 80 K and 420 K (Figure 2). First we investigated an ultrathin EC film with a mean thickness of around 5 Å, as calculated from the damping of Cu2p peaks, which was prepared by deposition on the Cu(111) sample held at 80 K. The film thickness corresponds to a coverage of between 1 and 2 monolayers. The two peaks in the C1s region in Figure 2a are related to the carbonyl carbon $C_{carbonyl}$ (290.8 eV) and the twocarbons of the ethylene group $C_{ethylene}$ (287.1 eV) of the adsorbed EC species. The nominal ratio of $C_{carbonyl}$:$C_{ethylene}$ of 1:2 is in good agreement with the experimentally determined aspect ratio of the peak areas of 1:1.9. Also in the XP O1s core level signals, two peaks are discerned. The more intense one is attributed to the oxygen atoms of the EC ring O_{ring} (E_B=534.3 eV) and the less intense one to the carbonyl oxygen $O_{carbonyl}$ (E_B=532.6 eV). Also here, the nominal amount of oxygen atoms of 2:1 in the molecule agrees well with the experimentally determined ratio of the peak areas within the limits of accuracy. The ratio of the total peak areas of the two carbon peaks and the total area of the two oxygen peaks is 1.1 (corrected by the different elemental sensitivity factors), which is almost identical to the molecular C/O ratio of 1. The XP C1s and O1s core level signals strongly support that under these conditions intact EC molecules are adsorbed on Cu(111). Hence, also the (2D) network, which was observed by STM, is composed of intact EC molecules. Note that at the low binding energy side at 530.8 eV an additional very weak signal (grey) is detected which originates from tantalum oxide of the sample holder.

Upon increasing the temperature, both the C1s and the O1s spectra change significantly. Representative spectra are shown in Figure 2, together with peaks of different decomposition products derived by deconvolution. For peak fitting of the variable temperature XP data, we fixed both the positions of the peaks of the intact EC and also the ratio of the peak areas. Furthermore, the positions of new peaks were fixed for all temperatures.

In the C1s region, the peak area decreases in the temperature interval between 80 K and ~200 K, which is attributed to a combination of desorption and decomposition of molecular species (see below). The latter is indicated by a shoulder growing in at the low binding energy side. At 170 K (Figure 2b), a consistent fit of the C1s signal (see above) requires two new peaks. The high BE side of the signal can be fitted by $C_{carbonyl}$ and $C_{ethylene}$ peaks, indicating that at that point still considerable amounts of intact adsorbed EC is present on the surface. The small shift of the two peaks to lower binding energies is explained by a final state effect, i.e., by a change in metallic screening of the EC photoion in the final state for EC molecules, which are in direct contact with the metal. The shoulder at the low binding energy side requires the addition of two more in the fit at binding energies of 285.5 eV (violet) and 284.3 eV (orange). Also in the O1s region the peak area decreases in this temperature range, and the appearance of a broad shoulder at lower BE points to the formation of new species. At 150 K (Figure 2b) the XP spectrum is fitted by $O_{carbonyl}$ and O_{ring}, which is, in agreement with the C1s signal, an indication for intact adsorbed EC species on the Cu(111) surface. Two additional peaks are needed to fit the spectrum, one at a slightly lower binding energy than $O_{carbonyl}$ at 532.5 eV (purple) and one at 530.9 eV (red). The decrease of the total peak area at 150 K in the C1s and O1s region by ~30 % and the observation of new peaks reflect the desorption of molecular entities on the one hand and the decomposition of EC on Cu(111) upon heating on the other hand.

Above ~200 K the new peaks are dominating the C1s and O1s regions. At 230 K (Figure 2c), the peak at 285.5 eV is most intense. Furthermore we found that the high binding energy side is not properly fitted by using the EC related peaks alone. Thus, a new peak in between the latter peaks at 288.8 eV (grey), was introduced to obtain a satisfactory fit. At this temperature the peak intensities of EC are weak and therefore only negligible amounts of residual EC are present on the surface. In the O1s region, the peaks related to intact EC were utilized for the fitting; however, the intensities are weak. At 210 K (Figure 2c) the new peak at 530.9 eV is dominating. Thus, also the O1s signals reveal that above ~200 K only a small amount of residual adsorbed EC is present on Cu(111). The O1s counterpart to the grey peak in the C1s region is most likely hidden underneath of one of the other O1s peaks.

Warming up the sample to 300 K (Figure 2d) is leading to an increase of the peak at 284.3 eV and a concomitant decrease of the peak at 285.5 eV. The peak at 530.9 eV dominates the O1s region, while the other peaks tend to vanish. At 300 K, no adsorbed EC can be detected by XPS.

Upon heating to 420 K, the compound at 284.3 eV persists, while the peak at 285.5 eV has almost disappeared. In the O1s region the peak at 530.9 eV fades.

In total, the spectra in Figure 2 demonstrate that the XP signals of intact EC on Cu(111) change significantly upon annealing from 80 K to around 420 K. Two new signals at binding energies of 284.3 eV and 285.5 eV grow in the C1s region, which are tentatively attributed to aliphatic C-C carbon and oxygen containing carbon moieties, respectively. The new peak at the high binding energy side at 288.8 eV can not be assigned unequivocally. Peaks in this binding energy region could be related, *e.g.*, to epoxy carbon (C-O-C), carbonyl carbon (C=O), or carboxylate carbon (O–C=O) [25], which would be also compatible with the hidden peak in the O1s region. The main new peaks in the O1s region at 532.5 eV and 530.9 eV might stem from oxygen bonded to carbon and adsorbed oxygen, respectively. At 420 K, the aliphatic C-C species persists on the surface, while a loss of oxygen is observed, which is manifested in the increasing C/O ratio. The latter is explained either by desorption of oxygen or dissolution into the bulk.

Overall, the data demonstrate that interaction of EC with a Cu surface leads to decomposition at temperatures far below room temperature, which is highly relevant for applications.

For further characterization of the (sub)molecular fragments additional measurements, employing, e.g., IR spectroscopy, are needed and planned for the future.

In conclusion, as a result of a variable temperature STM and XPS study we could identify the following main characteristics of the interaction of EC with an atomically flat Cu(111) surface under UHV conditions:

(1) Upon deposition of EC on the sample held at 80 K, EC adsorbs as intact molecule, forming highly ordered (2D) EC islands, which are symmetrically aligned to the underlying copper atomic lattice.

(2) The (2D) EC islands are stabilized by weak intermolecular interactions, and the individual molecules exhibit a low diffusion barrier on Cu(111), leading to the transformation into a mobile (2D) gas/(2D) liquid adlayer at room temperature.

(3) Annealing to higher temperature leads to competing desorption and decomposition of the EC molecules, at 200 K hardly any intact EC molecules are left on the surface. Decomposition intermediates / products are characterized by aliphatic C-C carbon, carbons bonded to oxygen and adsorbed oxygen O_{ad}. In addition, epoxy carbon C-O-C, carbonyl carbon C=O, carboxylate carbon O–C=O may be formed. At 420 K, almost only aliphatic carbon is left.

(4) Upon cool down (100 K) of a pre-annealed surface (180 - 200 K, 300 K), stable adsorbate islands were found to coexist with adsorbed oxygen atoms, where the former are attributed to aggregates of intermediate species (see (3)).

We expect that model studies as the present one, focussing on a mechanistic understanding of the interaction of individual compounds of battery electrolytes with model electrodes, can significantly contribute to the detailed understanding of the interactions at the electrode|electrolyte interface, which largely determines the functionality of real battery systems.

Notes and references

[a] *Helmholtz Institute Ulm, Albert-Einstein-Allee 11,D-89081 Ulm, Germany. Fax: +49 (0)731/50-25452; Tel: +49 (0)731/50-25451; E-mail: juergen.behm@uni-ulm.de*

[b] *Ulm University, Institute of Surface Chemistry and Catalysis, Albert-Einstein-Allee 47,D-89081 Ulm, Germany, Fax: +49 (0)731/50-25452; Tel: +49 (0)731/50-25451; E-mail: juergen.behm@uni-ulm.de*

† Electronic Supplementary Information (ESI) available: [experimental part]. See DOI: 10.1039/b000000x/

‡ These authors contributed equally

§ Present address: WATLab and Department of Chemistry, University of Waterloo, Waterloo, Ontario, N2L 3G1 Canada

1 V. Etacheri, R. Marom, R. Elazari, G. Salitra and D. Aurbach, *Energy Environ. Sci.*, 2011, **4**, 3243
2 J. B. Goodenough and Y. Kim, Chem. *Mater*. 2010, **22**, 587.
3 B. Scrosati and J. Garche, Journal of Power Sources, 2010, **195**, 2419.
4 A. Manthiram, *J. Phys. Chem. Lett.*, 2011, **2**, 176.
5 K. Xu, *Chem. Rev*., 2004, **104**, 4303.
6 P. Verma, P. Maire, and P. Novak, *Electrochim. Acta*, 2010, **55**, 6332.
7 P.B. Miranda and Y. R. Shen, *J. Phys. Chem. B*, 1999, **103**, 3292.
8 M. Moshkovich, M. Cojocaru, H.E. Gottlieb and D. Aurbach, *J. Electroanal. Chem*., 2001, **497**, 84.
9 T. Itoh, N. Anzue, M. Mohamedi, Y. Hisamitsu, M. Umeda and I.Uchida, *Electrochem. Commun.*, 2000, **2**, 743.
10 L. Yu, H. Liu, Y. Wang, N. Kuwata, M. Osawa, J. Kawamura and Shen Ye, *Angew. Chem.*, 2013, **125**, 5865.
11 D. Aurbauch, B. Markovsky, A. Rodkin, E. Levi, Y.S. Cohen, H.-J. Kim and M. Schmidt, *Electrochim. Acta*, 2002, **47**, 4291
12 K. Wang and P. N. Ross, Jr., *Surf. Sci*., 1996, **365**, 753
13 D. Becker, G. Cherkashinin, R. Hausbrand and W. Jaegermann, *Solid State Ionics*, 2013, **230**,83.
14 K. Ariga, T. Mori and J. P. Hill, *Langmuir*, 2013, **29**, 8459.
15 M. Olschewski, S. Knop, J. Lindner and P. Vöhringer, *Angew. Chem. Int. Ed*., 2013, **52**, 9634.
16 S. A. Claridge, W.-S. Liao, J. C. Thomas, Y. Zhao, H. H. Cao, S. Cheunkar, A. C. Serino, A. M. Andrews and P. S. Weiss, *Chem. Soc. Rev*., 2013,**42**, 2725.
17 S. De Feyter and F. C. De Schryver, *Chem. Soc. Rev*., 2003, **32**, 139.
18 J. V. Barth, *Annu. Rev. Phys. Chem.*, 2007, **58**, 375.
19 S. Berner, M. de Wild, L. Ramoino, S. Ivan, A. Baratoff, H.-J. Güntherodt, H. Suzuki, D. Schlettwein and T. A. Jung, *Phys. Rev. B*, 2003, **68**, 115410.
20 H. Yanagi, H. Mukai, K. Ikuta, T. Shibutani,T. Kamikado, S. Yokoyama and S. Mashiko, *Nano Lett.*, **2**, 601.
21 F. Buchner, E. Zillner, M. Röckert, Stefanie Gläßel, H.-P. Steinrück and H. Marbach, *Chem. Eur. J.*, 2011, **17**, 10226.
22. F. Wiame, V. Maurice and P. Marcus, *Surf. Sci.*, 2007, **601**, 1193.
23 F. Yang, Y. Choi, P. Liu, J. Hrbek, and J.A. Rodriguez, *J. Phys. Chem. C*, 2010, **114**, 17042.
24. P. Sautet, *Surf. Sci*., 1997, **374**, 406.
25. Y.-L. Huang, H.-W. Tien, C.-C. M. Ma, S.-Y. Yang, S.-Y. Wu, H.-Y. Liub and Y.-W. Mai, *J. Mater. Chem*., 2011, **21**, 18236.